

## **RHIC Longitudinal Parameter Revision**

Authors: J. Kewisch, V. Ptitsin, J. Rose, J. Wei

Editor: J. Wei

*Brookhaven National Laboratory, Upton, New York 11973*

### **Abstract**

The review of the longitudinal parameters during RHIC injection, acceleration, transition crossing, rebucketing and storage for gold and proton beams pointed to the need for revisions of the Design Manual baseline, with the new target values presented in this report. It was concluded that bunch rotations are needed in the AGS for gold as well as proton operations before the beams are injected into RHIC. For gold operation with nominal intensity, the acceptable range of 95% longitudinal bunch area is from 0.2 to 0.5 eV·s/u at injection, in comparison to the previous baseline value of 0.3 eV·s/u . Intra-beam scattering at injection and complications at transition will cause growth in longitudinal bunch size, resulting in increased bunch area before rebucketing. Consequently, at the upper limit of 0.5 eV·s/u a beam loss of about 3% is expected during rebucketing. The transfer from RHIC acceleration system to storage system is preferably performed at top energy to minimize possible sudden beam loss. For proton operation, the requirement on the initial bunch area is relaxed from the previous 0.3 eV·s to 0.5 eV·s . In either case, the change in collision performance is insignificant.

# 1 Introduction

Experimental conditions on the Relativistic Heavy Ion Collider (RHIC) desire[1] the rms bunch length of the beam to be about 22 cm during collision. This requirement will be met by operating the storage rf system at a frequency of 197 MHz. At nominal intensity, the beam size grows due to intra-beam scattering (IBS),[2] and the bunch length is ultimately confined by the width of the rf bucket. On the other hand, matching of the longitudinal bunch shape between AGS and RHIC requires a 28 MHz rf system in RHIC, which is used for injection, acceleration, and transition crossing. Over the years since the 1989 Conceptual Design Report,[3] several improvements to the operation and design of both the RHIC and AGS rf systems were introduced. The operation rf frequency in the AGS (from harmonic 12 to 8) and RHIC (acceleration system from harmonic 342 to 360, storage system from harmonic 2508 to 2520) have both been changed;[1] a first-order  $\gamma_T$  jump system has been designed,[6] reducing the chromatic nonlinearity and lattice perturbation (the first-order nonlinear momentum compaction factor[4]  $\alpha_1$  changed from +0.6 to -0.6).

In order to cross transition efficiently[4] and to transfer the bunches from the accelerating to the storage buckets with a minimum beam loss, the nominal 95% bunch area was baselined[1] in the 1997 Design Manual to be 0.3 eV·s/u for gold beams and 0.3 eV·s for proton beams. During the recent years, practice with gold beams at the AGS-RHIC injector complex[5] indicates that it will be difficult to achieve the previously specified small bunch area of 0.3 eV·s/u at nominal design intensity. The primary purpose of this report therefore was to investigate the impact of a larger bunch area at injection. Furthermore, it also represented the opportunity to review under these new conditions the complete ramping process including matching at injection, crossing efficiency at transition, scenarios of rebucketing from RHIC acceleration system to storage system, and IBS growth during storage.

In this introductory Section, we list tables of parameters for both baseline and revised/target machine operation. Table 1 shows relevant machine parameters. Table 2 shows the baseline parameter for both machine and beam during gold operation at injection and storage. The change of beam parameters from the beginning to the end of storage is mainly due to intra-beam scattering. Newly proposed and desired changes are listed as “target” values. Similarly, parameters for proton operation are listed in Table 3. Detailed discussions on gold and proton beam operations will be

Table 1: General RHIC Parameters.

Circumference	3833.845	m
Number of bunches/ring	60	
Number of crossing points	6	
Betatron tunes, H/V	28.18/29.18	
Transition energy, $\gamma_T$	22.89	
Bending radius, arc dipole	242.781	m
Acceleration system:		
rf harmonic number	360	
maximum voltage	600	kV
Storage system:		
rf harmonic number	2520	$= 7 \times 360$
maximum voltage	6	MV

presented in Sections 2 and 3, respectively. Conclusions and a discussion are given in Section 4.

## 2 Gold Operation

Except for protons, beams of all ion species are injected below transition energy. Among various ion species, intra-beam scattering is most severe for fully stripped gold ions ( $^{197}\text{Au}^{79+}$ ) at its design intensity of  $10^9$  per bunch. In this section, we discuss operational scenarios for gold ions. The results are applicable to all other ion species except for protons.

### 2.1 Injection

Matching between the rf systems of RHIC and AGS is essential in preserving the longitudinal bunch area at injection. The rf system in the AGS operates at harmonic 8 during gold operation with a voltage of about 300 kV. In order to preserve the longitudinal bunch area, the rf system in RHIC would need to operate at a voltage of 113 kV. The resulting bucket area would be  $0.66 \text{ eV}\cdot\text{s}/u$ , too small for a bunch with a 95% area of  $S = 0.5 \text{ eV}\cdot\text{s}/u$ . Therefore, a bunch rotation in AGS is necessary to change the aspect ratio of the bunch by a factor of about 1.6, matching the bunch into a RHIC bucket of  $1.5 \text{ eV}\cdot\text{s}/u$  created by an rf voltage of 600 kV. Since during every AGS cycle 4 bunches are accelerated, but only one bunch is extracted at a

Table 2: Baseline and target parameters for RHIC gold operation. If not specified, the target value is the same as the corresponding baseline value.

Quantity	unit	Injection		Store (begin)		Store (end)	
		baseline	target	baseline	target	baseline	target
Kinetic Energy	GeV/u	10.4		100		100	
Relativistic factor, $\gamma$		12.6		108.4		108.4	
$\beta^*$ at IP	m	10		2	1 <sup>a</sup>	2	1 <sup>a</sup>
Ions per bunch, $N_b$		10 <sup>9</sup>		10 <sup>9</sup>		6×10 <sup>8b</sup>	
95% bunch area, $S$	eV·s/u	0.3	0.2–0.5	0.3	0.3–0.7	1.1	
95% emittance, $\pi\epsilon_N$	$\pi$ mm·mr	10		15		43	
RF frequency	MHz	28.2		197.1		197.1	
RF voltage	kV	215 <sup>c</sup>	600 <sup>d</sup>	6000		6000	
RF bucket area	eV·s/u	0.9	1.5	1.2		1.2	
RF bucket full width	m	10.7		1.52		1.52	
	ns	35.6		5.1		5.1	
RF bucket height	10 <sup>-3</sup>	1.7	2.9	1.8		1.8	
Synchrotron freq.	Hz	106 <sup>e</sup>	178 <sup>e</sup>	326		326	
Synchrotron tune	10 <sup>-3</sup>	1.4	2.3	4.2		4.2	
RMS bunch length	m	0.72	0.55–0.88	0.11	0.11–0.17	0.22	
	ns	2.4	1.9–2.9	0.37	0.37–0.57	0.74	
RMS $\Delta p/p$	10 <sup>-4</sup>	3.6	4.7–7.4	4.2	4.2–6.4	8.8	
$\mathcal{L}$	10 <sup>26</sup> cm <sup>-2</sup> s <sup>-1</sup>			8.1	16.2–15.6	1.0	1.8–1.7
$\mathcal{L}_{integral}$ (10 hour)	$\mu$ b <sup>-1</sup>					7.9	15.0–14.6

- (a) At 6 and 8 o'clock interaction point (IP), the target  $\beta^*$  is 1 m, and the nominal  $\beta^*$  is 2 m. At 2, 4, 10, and 12 o'clock IP, the  $\beta^*$  is larger or equal to 2 m.[7]
- (b) Particle loss occurs mostly due to intra-beam scattering.
- (c) Originally, the RHIC acceleration voltage was determined by the AGS-RHIC injection matching assuming a rf harmonic number of 12 (frequency 4.45 MHz, voltage 320 kV) in AGS. Currently, with AGS operating at harmonic 8 and voltage 320 kV, the RHIC matching voltage is 113 kV. The corresponding bucket area is 0.66 eV·s/u .
- (d) This value is chosen to minimize IBS growth in longitudinal bunch area at injection. A reversible bunch rotation is required in AGS before the beam is extracted. Otherwise, with AGS operating with harmonic 8 at 300 kV, the matching voltage of the RHIC acceleration system is 113 kV. The resulting rf bucket area is only 0.66 eV·s/u , too small for a bunch of 0.5 eV·s/u area.
- (e) During the acceleration ramp when the beam is near transition, the synchrotron tune will cross the potentially hazardous power-supply frequency of 60 Hz.

Table 3: Baseline and target parameters for RHIC proton operation. If not specified, the target value is the same as the corresponding baseline value.

Quantity	unit	Injection		Store (begin)		Store (end)	
		baseline	target	baseline	target	baseline	target
Kinetic Energy	GeV/u	28.3		250.7		250.7	
Relativistic factor, $\gamma$		31.2		268.2		268.2	
$\beta^*$ at IP	m	10		2	1	2	1
Ions per bunch, $N_b$		$10^{11}$	$2 \times 10^{11a}$	$10^{11}$	$2 \times 10^{11}$	$10^{11}$	$2 \times 10^{11}$
95% bunch area, $S$	eV·s	0.3	0.5	0.3	0.5	1.2	1.4
95% emittance, $\pi\epsilon_N$	$\pi\text{mm}\cdot\text{mr}$	20		20		29	27
RF frequency	MHz	28.2		197.1		197.1	
RF voltage	kV	196 <sup>b</sup>	170 <sup>b</sup>	6000		6000	
RF bucket area	eV·s	4.8	4.5	2.9		2.9	
RF bucket full width	m	10.7		1.52		1.52	
	ns	35.6		5.1		5.1	
RF bucket height	$10^{-3}$	3.7	3.4	1.8		1.8	
Synchrotron freq.	Hz	45 <sup>c</sup>	42 <sup>c</sup>	333		333	
Synchrotron tune	$10^{-3}$	0.58	0.54	4.3		4.3	
RMS bunch length	m	0.38	0.51	0.070	0.091	0.14	0.15
	ns	1.3	1.7	0.24	0.30	0.48	0.51
RMS $\Delta p/p$	$10^{-4}$	4.1	5.1	2.6	3.4	5.1	5.7
$\mathcal{L}$	$10^{31} \text{ cm}^{-2}\text{s}^{-1}$			1.5	12	1.1	7.6
$\mathcal{L}_{integral}(10 \text{ hour})$	$\text{pb}^{-1}$					0.45	3.3

- (a) The nominal intensity is  $10^{11}$  protons per bunch. A higher intensity is desired especially for polarized proton operation.
- (b) Since the injection occurs near transition, the RHIC matching voltage is only 19 kV, comparable to the induced voltage from beam loading. In order to avoid complications, a reversible bunch rotation is needed in AGS, resulting in the corresponding RHIC voltages.
- (c) At  $V_{acc} = 170$  kV, the synchrotron frequency will not cross the 60 Hz power-supply frequency during the acceleration ramp. However, this potentially hazardous power-supply frequency may be crossed if a higher voltage is used for proton acceleration.

time into RHIC, this bunch rotation process needs to be reversible to avoid bunch filamentation.<sup>1</sup>

Due to fast IBS growth, RHIC injection needs to be completed in about 2 minutes to avoid excessive emittance growth. At injection,[9, 10] the transverse beam temperatures are much higher than the longitudinal temperature,

$$\left\langle \frac{\sigma_x}{\beta_x} \right\rangle \approx \left\langle \frac{\sigma_y}{\beta_y} \right\rangle \gg \left( \frac{1}{\gamma} - \frac{1}{\gamma_T} \right) \sigma_p,$$

where  $\langle \rangle$  indicates an average over the circumference,  $\sigma_x$  and  $\sigma_y$  are the rms transverse beam sizes, and  $\sigma_p$  is the rms momentum deviation  $\Delta p/p$ . During the initial two minutes[11, 9] of injection, the growth in longitudinal bunch area can be significant. Fig. 1 shows[12] the 95% bunch area at the end of injection as a function of the initial

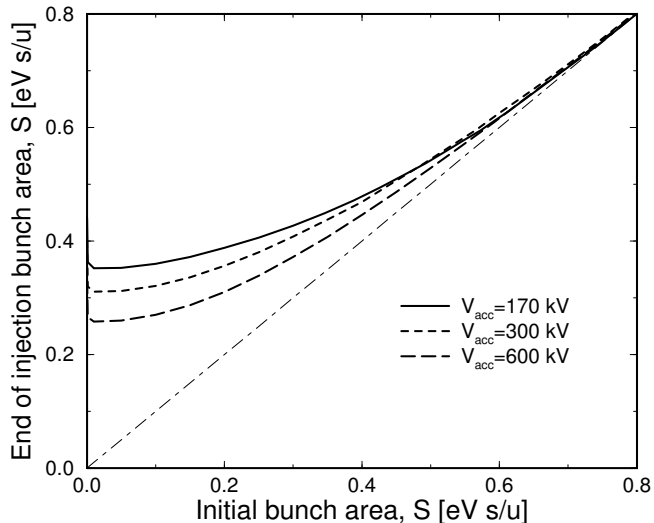


Figure 1: Growth in bunch area of a gold beam due to intra-beam scattering during the initial 2-minute injection period.

bunch area. In order to minimize this growth, the maximum rf voltage of 600 kV is chosen to lower the longitudinal temperature. Fortunately, the growth in transverse emittance due to IBS is negligible ( $< 1\%$ ).

<sup>1</sup>A proof-of-principle experiment has been successfully performed[8] in AGS.

## 2.2 Transition Crossing

Due to the slow ramp of superconducting magnets, both chromatic nonlinear effects and beam self-field effects are significant at transition. Transition crossing in RHIC requires a  $\gamma_T$  jump to effectively increase the crossing rate. The quadrupole correctors are excited to vary  $\gamma_T$  of the lattice by  $\pm 0.4$  units in 60 ms. Even with the  $\gamma_T$  jump, growth in longitudinal bunch area is expected during crossing. Fig. 2 shows the 95%

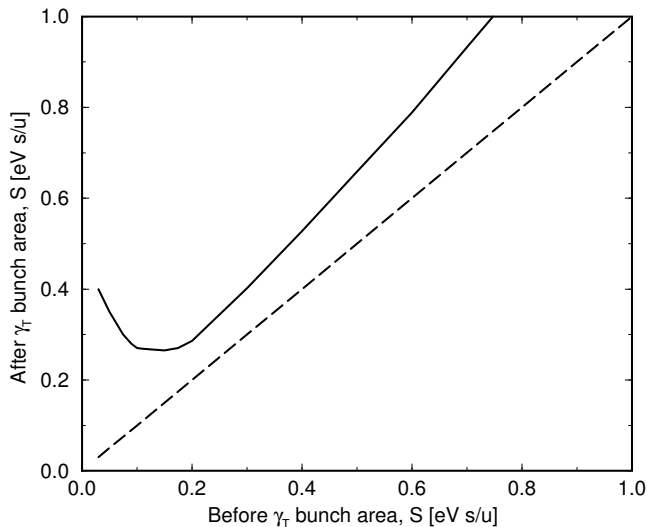


Figure 2: Growth in bunch area of a gold beam at transition in the presence of a  $\gamma_T$  jump of  $\pm 0.4$  units in 60 ms.

bunch area after transition as a function of that before transition. At small bunch area  $S$ , single-bunch instability starts[4] to occur when  $S$  is below about 0.1 eV·s/u at the nominal intensity of  $10^9$  ions per bunch. On the other hand, at large bunch area the proposed  $\gamma_T$  jump becomes inadequate[13] when  $S$  is above about 0.6 eV·s/u.

Effects of chromatic nonlinearity depend strongly on the machine lattice. The growth in bunch area is approximately proportional to the factor  $(\alpha_1 + 1.5)$ , where  $\alpha_1$  is the first-order nonlinear momentum compaction factor.[4] During the entire period of the  $\gamma_T$  jump,  $\alpha_1$  varies between  $-0.5$  and  $-0.7$ .

With an initial area of 0.5 eV·s/u at injection, the bunch area is expected to be about 0.52 eV·s/u before transition (Fig. 1), and is near 0.7 eV·s/u after transition (Fig. 2). In the presence of the  $\gamma_T$  jump, no beam loss is expected to occur.

## 2.3 Rebucketing

After being accelerated to the top energy with the acceleration system, the beam must be handed over to the storage system for collision. This process is called “rebucketing”. The objectives for a successful rebucketing are

- (a) minimization of particle loss, and
- (b) minimization of the energy deposited in the magnets by particle loss.

On the other hand, it is not an objective to produce gold bunches that are considerably shorter than the storage bucket because intra-beam scattering will void such an effort in a short time.

With a bunch area after transition from 0.3 to 0.7 eV·s/u , the beam has before the rebucketing a 95% length from 1.4 to 2.2 m, compared with the bucket width of 1.52 m. In order to avoid excessive particle loss, a bunch rotation is necessary to shorten the bunch length.

A bunch rotation consists of several steps. First, the synchronous phase of the acceleration system is shifted to the unstable fixed point for a short time. The bunch will stretch in the longitudinal phase space, as shown in Fig. 3. The phase of the

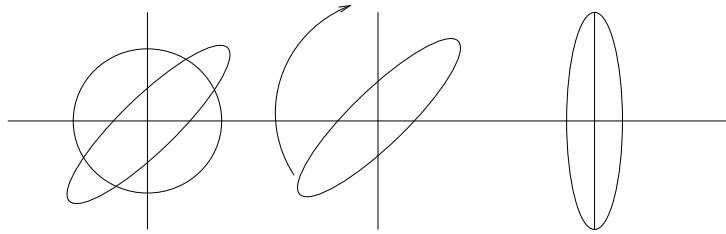


Figure 3: Bunch shortening by a rotation using the unstable fixed point shown in the longitudinal phase space.

acceleration system is then returned to the stable fixed point. The stretched bunch rotates in phase space and becomes short after 3/8th of a synchrotron period. At this point the storage system is turned on and captures the bunch.

If it were not for the nonlinear motion, the beam would be matched perfectly to the receiving bucket by adjusting the stretch time to obtain the matching bunch aspect ratio.[4] Unfortunately, the synchrotron tune decreases with the particles’ amplitude and the bunch is deformed during the 3/8th rotation to an S-shape (Fig. 4). Particles in the tips of this “S” may be outside of the receiving bucket and thus lost.



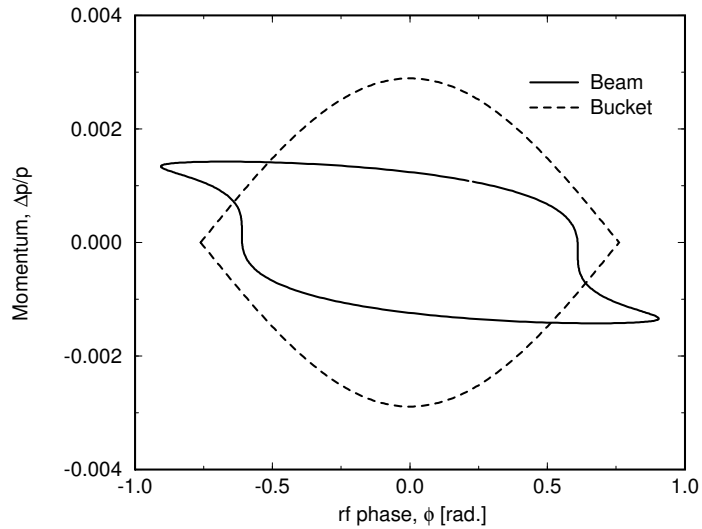


Figure 4: Bunch deformation caused by nonlinear longitudinal motion. The solid line indicates the beam contour, and the dashed line indicates the rf bucket created by the 197 MHz storage system.

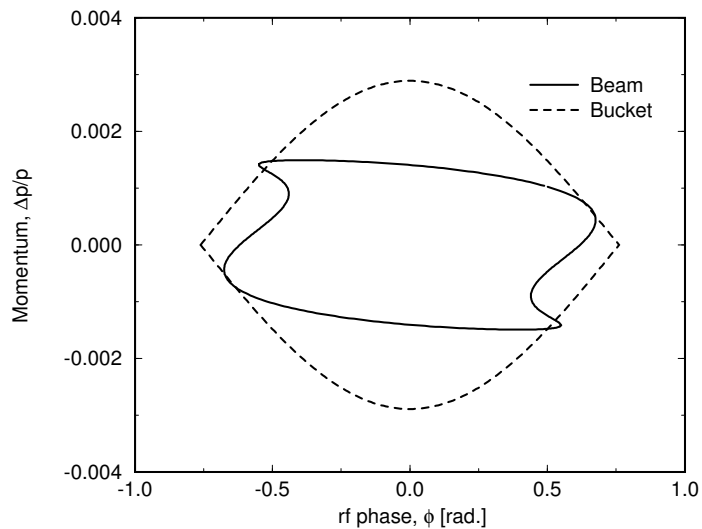


Figure 5: Increased longitudinal acceptance through an over-rotation in comparison with Fig. 4. The solid line indicates the beam contour, and the dashed line indicates the rf bucket created by the 197 MHz storage system.

It is therefore necessary to constrain from stretching of the beam and trade off the resulting mismatch against the nonlinear deformation. A turn-by-turn tracking program was used to simulate and optimize the rebucketing process by varying both the stretch-time and the rotation time. The program tracks 100,000 particles which are initially placed in a Gaussian-like<sup>2</sup> distribution. By rotating slightly more than 3/8th of a synchrotron period it is possible to accommodate larger nonlinear deformation (Fig. 5). After the rebucketing the program follows the particles for 8 synchrotron periods and evaluates particle loss (defined here as particles outside of the rf bucket).

Due to complications in transition crossing, rebucketing needs to be performed above transition. Since the growth in bunch area is negligible during the acceleration process, and since the limiting factor is the size of the storage bucket area, rebucketing should occur at energies at which the bucket area is large, i.e. either at top energy ( $\gamma = 108$ ) or shortly after transition crossing, as shown in Fig. 6. In the following

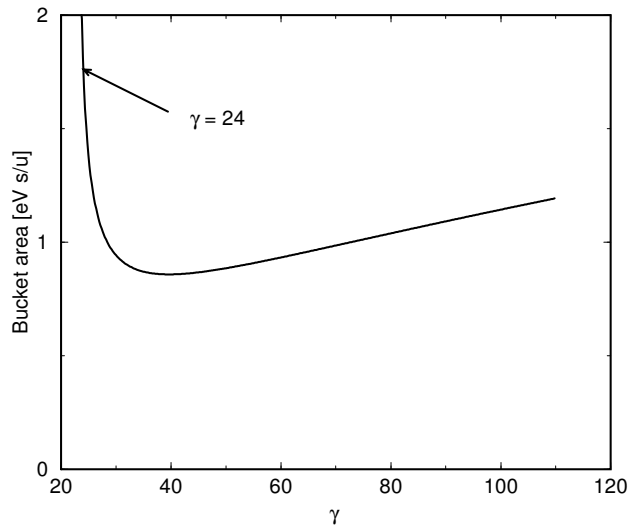


Figure 6: Bucket area as a function of the relativistic factor  $\gamma$  for a gold beam.

subsections, we discuss the results of these two scenarios respectively.

### 2.3.1 Rebucketing at top energy

Fig. 7 shows the gold beam loss due to rebucketing as a function of the bunch area

---

<sup>2</sup>Due to intra-beam scattering at injection, a diffusive process, the bunch shape is Gaussian-like.

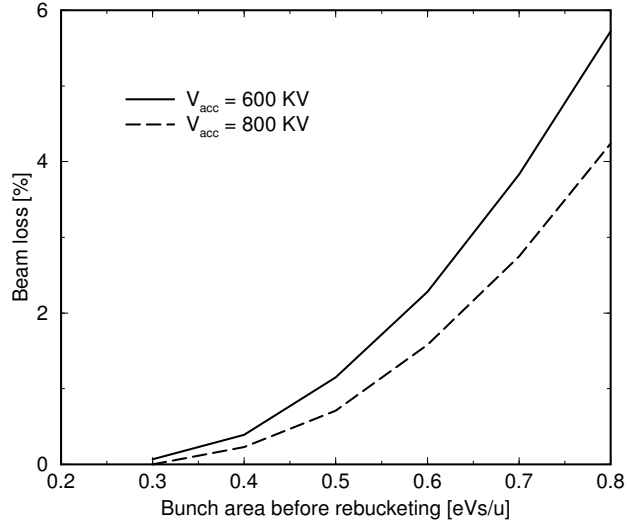


Figure 7: Beam loss as a function of pre-rebucketing bunch area at acceleration system voltages of 600 and 800 kV, respectively.

before rebucketing. With an initial bunch area of  $0.5 \text{ eV}\cdot\text{s/u}$  at injection at the nominal intensity, the pre-rebucketing area is about  $0.7 \text{ eV}\cdot\text{s/u}$ . For the nominal case (solid line) with the rf peak voltage at 600 kV for the acceleration system and 6 MV for the storage system, the predicted beam loss is about 3.5% for this  $0.7 \text{ eV}\cdot\text{s/u}$  beam, compared with a zero loss for a pre-rebucketing bunch area of  $0.3 \text{ eV}\cdot\text{s/u}$  ( $0.2 \text{ eV}\cdot\text{s/u}$  at injection).

Since the nonlinear synchrotron motion causes beam loss, it helps to increase the peak voltage of the acceleration system. At a possibly achievable voltage of 800 kV (dashed line in Fig. 7), we will have 1/3 less beam loss. Table 4 summarizes the dependence of beam loss on the peak rf voltage. Rows 1 – 3 shows the influence of the acceleration system voltage.

Each of the rings in RHIC has 3 storage system cavities and shares another 4 common cavities with the other ring. In order to simplify the operations (rebucket one ring at a time) it was investigated how large the losses are if the common cavities are not used. The remaining cavities produce a peak voltage of 3 MV. Rows #4 and #5 show that the beam loss approximately doubles.

Increasing the voltage of the storage system gives little improvement (row #6), since the bucket height of the storage system is already larger than the height of the

Table 4: Longitudinal simulation results for rebucketing of gold ions at top energy.

#	$\gamma$	$V_{acc}$ [kV]	$V_{sto}$ [MV]	Loss [%]
1	108	600	6	3.5
2	108	800	6	2.5
3	108	1,000	6	1.9
4	108	600	3	5.3
5	108	800	3	4.3
6	108	600	8	3.1

acceleration system.

### 2.3.2 Rebucketing near transition energy

In order to minimize the energy deposited into the magnets by the lost particles, it is attractive to rebucket the beam at low energies. We consider to rebucket at  $\gamma = 24$ , sufficiently far away from transition ( $\gamma_T = 22.89$ ) to avoid complications due to the non-adiabatic longitudinal motion and self-field mismatch.[4]

First the good news: rebucketing at  $\gamma = 24$  produces less particle loss, even if it is done “on the fly”, i.e. during acceleration. The bad news becomes obvious when we plot the bucket area as a function of  $\gamma$  (Fig. 6). The bucket area at  $\gamma = 24$  is larger than that at top energy ( $\gamma = 108$ ), but decreases to a minimum at  $\gamma \approx 40$ . Particles that survive the rebucketing may get lost during the ramp. Furthermore, slow instabilities near transition[15, 16] may occur if the rebucketing is not performed promptly.

For a quick answer, the simulations were performed at  $\gamma = 24$  with a reduced storage system voltage, so that the bucket area is the same as it would be with full voltage at  $\gamma = 40$ . The result is shown in Table 5. The beam loss is in all cases comparable to a rebucketing at top energy.

Rebucketing after transition is technically more difficult than at top energy because it is done during acceleration. Although the energy deposited by the lost

Table 5: Longitudinal simulation results for rebucketing of gold ions at  $\gamma = 24$ .

#	$\gamma$	$V_{acc}$ [kV]	$V_{sto}$ [MV]	Loss [%]
1	24	600	6	3.7
2	24	800	6	2.3
3	24	600	3	5.7
4	24	600	8	3.8

particles is smaller and spread out over a certain period, any loss will hit the machine aperture during the subsequent acceleration, as contrast to drifting as a coasting beam background without hitting the aperture when the rebucketing is performed at top energy. It is the current understanding that a loss is preferred[14] to occur in such a way that particles outside of the rf bucket coasts around the ring as a less-harmful background, as contrasted to a sudden loss on some magnets which may cause quenches in superconducting magnets. For this reason, rebucketing is preferred to be performed at top energy when beam acceleration is completed. Therefore, rebucketing near transition should be considered only as an alternative.

## 2.4 Collision

Due to intra-beam scattering, the gold beam fills the entire rf bucket within the first hour of storage at the top energy. Subsequently, particles diffuse into the unstable region[2] becoming coasting beam background. Fig. 8 demonstrates the evolution of gold beam normalized 95% transverse emittances and rms bunch length during a 10-hour storage for bunch areas of  $S = 0.7$  and  $0.3$  eV·s/u at the beginning of storage. A full coupling in the transverse plane is assumed that allows a significant reduction of growth of the horizontal emittance.[9] As seen from the figures, an increase of the longitudinal bunch area from  $0.3$  to  $0.7$  eV·s/u does not significantly change the IBS behaviour of the beam: transversely the emittance grows by a factor of 2.5 in 10 hours and longitudinally particles fill up the bucket within the first hour.

At  $\beta^* = 2$  m, the intensity loss of the gold beam is about 45% in 10 hours, mostly

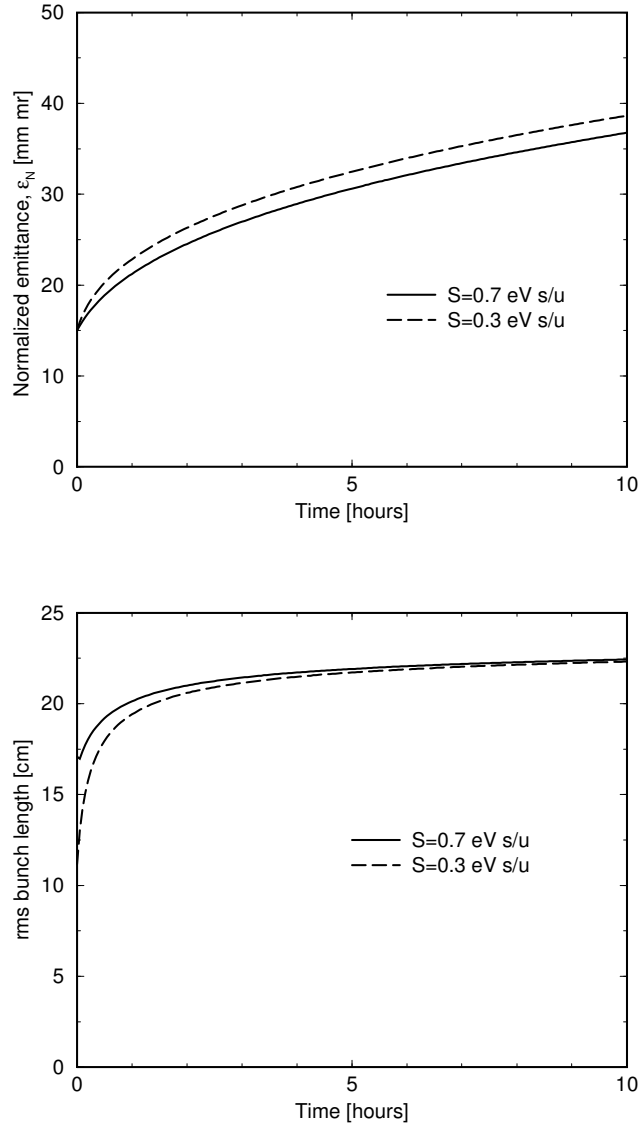


Figure 8: Evolution of the normalized 95% transverse emittances and rms bunch length of a gold beam during storage with an initial  $S = 0.7$  and  $0.3$  eV·s/u and with  $V_{sto} = 6$  MV.

due to IBS diffusion with particles escaping outside of the rf bucket.[2] Reducing the value of  $\beta^*$  to 1 m leads to an increase of particle losses due to Coulomb induced processes upon collisions[17], but this effect is small (about 10%) compared with intra-beam scattering. Assuming that beam loss due to transverse dynamic aperture limitations is negligible, Fig. 9 shows the increase of integrated luminosities (a factor

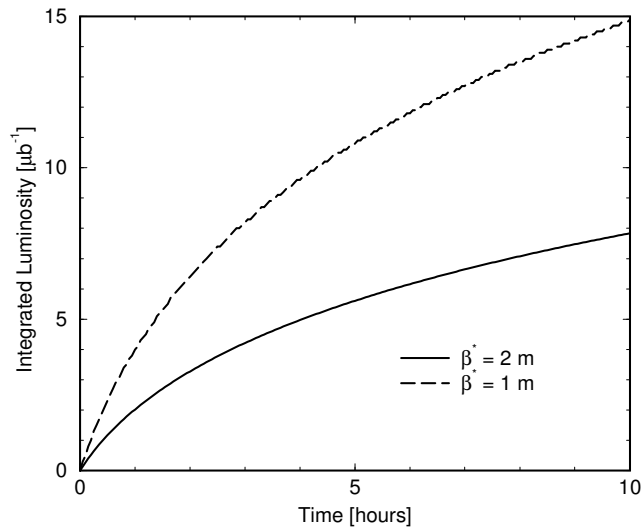


Figure 9: Luminosity variation during storage of a gold beam of  $S = 0.5$  eV·s/u initial longitudinal bunch area.

of 1.9) of  $\beta^* = 1$  m upon that of  $\beta^* = 2$  m. The luminosity performance is insensitive to the initial bunch area.

### 3 Proton Operation

Proton beams are injected into RHIC above transition at  $\gamma = 31.2$ . Compared with gold beams, the operation is expected to be less complicated. A 95% bunch area of 0.5 eV·s is used for investigation.

#### 3.1 Injection

The proton beam is injected from the AGS and captured with the 28 MHz RHIC acceleration system. Since the injection occurs near transition energy, the matching

voltage of the RHIC acceleration system is only 19 kV when the AGS operates with harmonic 8 at 300 kV. At this low voltage, the effect of beam loading is expected to be strong. In order to avoid complications, a reversible bunch rotation is again needed in AGS before the beam is extracted for RHIC injection. Table 3 lists the corresponding injection parameters.

Intra-beam scattering does not cause noticeable emittance increase for protons at injection. The growths in transverse and longitudinal directions are approximately

$$\left| \frac{\Delta \epsilon_x}{\epsilon_x} \right| \approx \left| \frac{\Delta \epsilon_y}{\epsilon_y} \right| \approx 0.1\%, \text{ and } \frac{\Delta S}{S} \simeq 1.5\%$$

during the initial two minutes of injection period.

### 3.2 Rebucketing

Fig. 10 shows the stationary bucket area as a function of  $\gamma$  for protons. Rebucketing

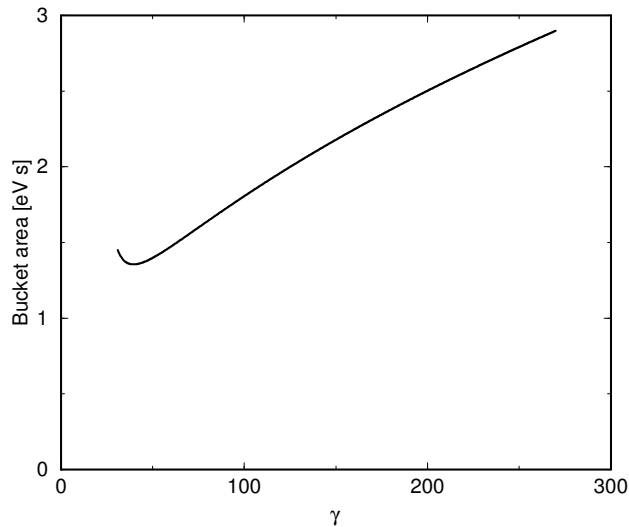


Figure 10: Bucket area as a function of the relativistic factor  $\gamma$  for a proton beam.

should be performed at top energy after the acceleration is completed. The bucket area per nucleon at top energy is about 2 1/2 times larger than that of gold. No beam loss is expected during proton rebucketing.



### 3.3 Collision

Compared with gold beams, effects of intra-beam scattering for proton beams is much less significant. Evolution of the proton normalized 95% transverse emittances during a 10-hour storage are shown in Fig. 11 for  $S = 0.5$  and  $0.3$  eV·s bunch areas,

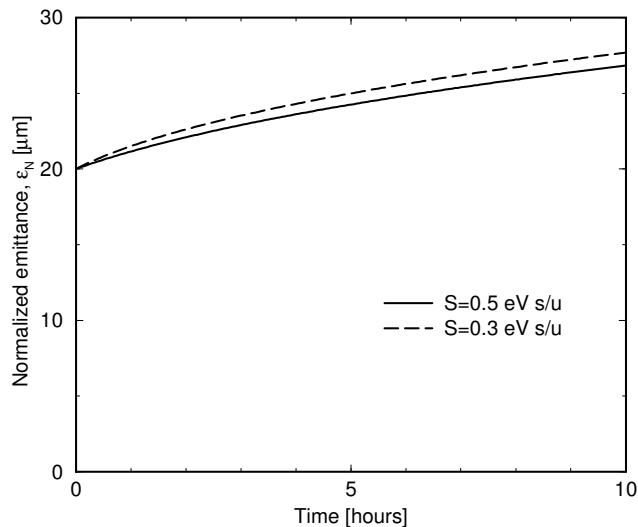


Figure 11: Evolution of the normalized 95% transverse emittances and rms bunch length of a proton beam during storage with an initial  $S = 0.5$  and  $0.3$  eV·s/u and with  $\gamma = 268.2$ ,  $\beta^* = 2$  m,  $N_b = 10^{11}$ ,  $V_{sto} = 6$  MV.

respectively, at a nominal intensity of  $N_b = 10^{11}$  and an rf voltage of  $V_{sto} = 6$  MV. A full transverse coupling is again assumed. Obviously, beam evolution at storage is insensitive to the initial bunch area. The transverse emittances grows by about 40% during 10 hours to about  $29 \pi\text{mm}\cdot\text{mr}$ . The longitudinal bunch area grows by a factor of 2.2, but is still considerably less than the bucket area. Particle loss due to IBS is negligible.

At a higher intensity of  $2 \times 10^{11}$  per bunch, beam loss due to intra-beam scattering is still negligible. Fig. 12 shows the rms bunch length versus the storage time. Table 6 summarizes the emittance growths, particle losses and integral luminosities for a 10-hour storage at bunch intensities of  $N_b = 1 \times 10^{11}$  and  $N_b = 2 \times 10^{11}$ , and at rf voltage  $V_{sto} = 3$  MV and  $V_{sto} = 6$  MV, respectively.

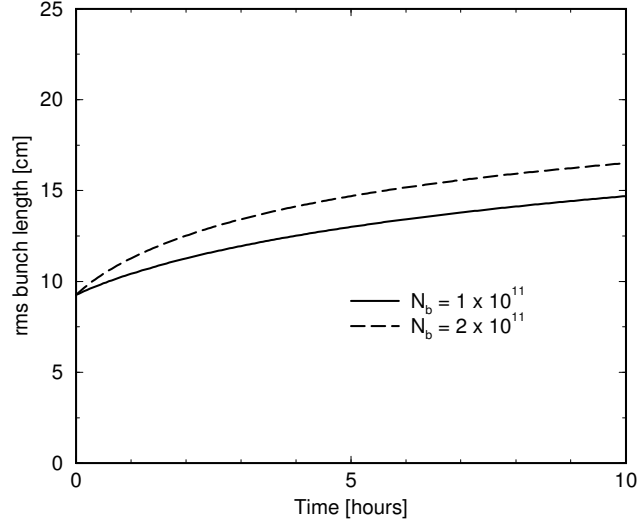


Figure 12: Evolution of the rms bunch length of a proton beam during storage with an initial  $S = 0.5$  eV·s and with  $\gamma = 268.2$ ,  $\beta^* = 2$  m, and  $V_{sto} = 6$  MV.

Table 6: Final transverse emittance, longitudinal bunch area, and integrated luminosity for a 10-hour storage at various bunch intensities and rf voltages with an initial bunch area of  $S = 0.5$  eV·s/u and an emittance of  $\epsilon_N = 20\pi$ mm·mr at  $\beta^* = 2$ m.

unit		$N_b = 1 \times 10^{11}$		$N_b = 2 \times 10^{11}$	
		$V_{sto} = 3$ MV	$V_{sto} = 6$ MV	$V_{sto} = 3$ MV	$V_{sto} = 6$ MV
$\pi \epsilon_N$	$\pi$ mm·mr	27	29	31	33
$S$	eV·s	1.4	1.2	1.6	1.6
$\Delta N_b/N_b$		0	0	1%	0
$\mathcal{L}_{integral}$	pb <sup>-1</sup>	0.45	0.45	1.6	1.6

## 4 Conclusions and Discussion

This report summarizes the proposed revisions to the longitudinal parameters for both gold and proton operations. With the bunch area of both gold and proton beams increased from 0.3 eV·s/u to up to 0.5 eV·s/u at injection, instabilities are less likely to occur. Furthermore, growth due to intra-beam scattering at injection is reduced. If a  $\gamma_T$  jump of  $\pm 0.4$  units in 60 ms is performed, the growth in longitudinal bunch area is confined to about 25%. The constraint is set by the transfer efficiency from the RHIC acceleration system to the storage system (rebucketing process).

Bunch rotations are needed in AGS for both gold and proton operations before the beams are injected into RHIC. The transfer from RHIC acceleration system to storage system is preferably performed at top energy to avoid possible sudden beam loss that may cause magnet quench. For gold operation under nominal condition, the acceptable range of 95% longitudinal bunch area is from 0.2 to 0.5 eV·s/u at injection, in comparison to the previous baseline value of 0.3 eV·s/u. Intra-beam scattering at injection and complications at transition will cause growth in longitudinal bunch size, resulting in increased bunch area before rebucketing. Consequently, at the upper limit of 0.5 eV·s/u a beam loss of about 3% is expected during rebucketing. For proton operation, the requirement on the initial bunch area is relaxed from the previous 0.3 eV·s to 0.5 eV·s. In either case, the change in collision performance is insignificant.

Baseline and revised/target parameters are summarized in Tables 2 (for gold) and 3 (for proton), respectively.

## Acknowledgments

We would like to thank J.M. Brennan, H. Hahn, M. Harrison, S. Peggs, and A. Stevens for many useful discussions. Work performed under the auspice of the U.S. Department of Energy.

## References

- [1] *RHIC Design Manual* (Brookhaven National Laboratory, Upton, September 1997).
- [2] J. Wei, *Stochastic Cooling and Intra-Beam Scattering in RHIC*, Proc. Workshop on Beam Cooling and Related Topics, Montreux, p.132, 1994 (CERN 94-)

- 03); J. Wei and A.G. Ruggiero, *Beam Life-Time with Intrabeam Scattering and Stochastic Cooling*, Proc. of the 1991 IEEE PAC, San Francisco, 1869 (1991).
- [3] *Conceptual Design of the Relativistic Heavy Ion Collider* (Brookhaven National Laboratory, Upton, May 1996).
- [4] J. Wei, *Longitudinal Dynamics of the Non-Adiabatic Regime on Alternating-Gradient Synchrotrons*, Ph. D. dissertation, Stony Brook, New York (1990); revised 1994.
- [5] J.M. Brennan, *AGS – Injector Upgrade*, Talk at the Machine Advisory Committee Review, March 6-7, 1997.
- [6] S. Peggs, S. Tepikian, D. Trbojevic, *A First Order Transition Jump at RHIC*, Proc. 1993 Part. Accel. Conf., (Washington D.C., 1993), p.168.
- [7] S. Peggs, V. Ptitsin, S. Tepikian, P. Thompson, D. Trbojevic, *Interaction Region Closed Orbits*, RHIC Accelerator Physics Note AP/135 (1997).
- [8] J.M. Brennan, AGS Machine Study Report # 344.
- [9] J. Wei, *Evolution of Hadron Beams under Intrabeam Scattering*, Proc. 1993 Part. Accel. Conf., Washington, D.C. (1993) p.3653.
- [10] W. Fischer, W.W. Mackay, S. Peggs and J. Wei, *Emittance growth in RHIC during injection*, RHIC/AP/112, (1996).
- [11] A. Piwinski, Proc. of the 9th Intern. Conf. on High Energy Accel., 405 (1974).
- [12] This result is obtained with the computer program *store* originally written by S. Peggs.
- [13] J. Wei and S. Peggs, *Transition-Energy Crossing with a  $\gamma_t$ -Jump*, Proc. European Accelerator Conference, London, U.K., June 26-July 1 (1994) p. 973 - 975.
- [14] A. Stevens, Private Communications (1997).
- [15] H. G. Hereward, RL-74-062, EPIC/MC/48, Rutherford Lab, 1974.
- [16] D. Boussard and T. Linnecar, 2nd European Part. Accel. Conf., 1560 (Nice, 1990).
- [17] A.J. Baltz, M.J. Rhoades-Brown and J. Weneser, Phys.Rev. E, **54**, 4233 (1996).